Chapter 4
Water Depollution Using Ferrites Photocatalysts

Virender K. Sharma, Chun He, Ruey-an Doong, and Dionysios D. Dionysiou

Abstract The presence of organic pollutants and pathogenic microorganisms in water has become an increasing concern throughout the world. Heterogeneous photocatalytic technologies have been applied to control the organic pollutants and microorganisms in water. Development of narrow band-gap photocatalysts which function in the visible light remains a challenge in the wastewater treatment processes. Spinel ferrites has attracted a remarkable attention because of a relatively narrow band gap of about 2.0 eV, which has considerable photo-response in the visible light region. This chapter reviews recent advances in ferrites and the application of visible light photocatalysts to the remediation of contaminants such as H_2S, phenols, and dyes in water. Recent development in synthesis and characterization of ferrite and hybrid ferrites with other semiconductors is reviewed. The applications of ferrites in photocatalytic conversion of visible solar energy to generate e^-/h^+, which in turn produce reactive oxygen species through redox processes for the degradation of the pollutants in water, are demonstrated. We discuss the enhanced visible photocatalytic activity of ferrites by doping with metals and combing with

V.K. Sharma (✉)
Center of Ferrate Excellence and Chemistry Department, Florida Institute of Technology, 150 West University Boulevard, Florida 32901, USA
e-mail: vsharma@fit.edu

C. He
School of Environmental Science and Engineering, Sun Yat-sen University, Guangzhou 510275, China

R.-a. Doong
Department of Biomedical Engineering and Environmental Sciences, National Tsing Hua University, Hsinchu 30013, Taiwan

D.D. Dionysiou
Environmental Engineering and Science Program, 705 Engineering Research Center, University of Cincinnati, Cincinnati, OH 45221-0012, USA

E. Lichtfouse et al. (eds.), *Green Materials for Energy, Products and Depollution*, Environmental Chemistry for a Sustainable World 3, DOI 10.1007/978-94-007-6836-9_4,

other photocatalysts. Moreover, the addition of H_2O_2 to ferrite either in dark or visible light irradiation indicates the enhanced degradation efficiency for organic pollutants.

Keywords Water pollution • Photocatalyst • ferrite • H_2S • Phenols • Dyes • H_2O_2 • Surfactant • Agrochemical • Glyphosate

Contents

4.1 Introduction

Freshwater is a precious resource on earth and is critical to sustain life. In many regions of the world, daily need of water is not met. According to World Health Organization (WHO), more than 880 million people in the world do not have access to potable water (WHO 2010). Water contamination caused death to 1.8 million children from diarrhea every year (WHO 2010). Water scarcity can also affect ecosystem as numerous species might not be able to cope with decrease in availability of freshwater. One of the greatest challenges in this century is to provide access to clean water. The development of nanotechnology in the past decade offers prospects of meeting challenges of safe and sustainable water demand (Di Paola et al. 2012; Qu et al. 2012). Furthermore, a combination of nanotechnology and solar energy may lead to innovative water purification technologies.

One of the well studied technologies to clean water is the photocatalytic remediation (Di Paola et al. 2012; Rajeshwar 2011; Rajeshwar et al. 2012). The photocatalytic processes on bare semiconductor titanium dioxide (TiO_2) have been studied for several decades, but TiO_2 is only active under UV irradiation ($\lambda < 400$ nm) (Abe 2011; Chen et al. 2011; Hoffmann et al. 1995; Li and Liu 2011; Serpone et al. 2012; Tao et al. 2011). The solar spectrum has very small fraction of incoming light in the UV region (ca. 4 %). A use of all the UV light would result in only 2 % solar conversion efficiency (Abe 2011). Comparatively, the portion of visible light ($400 < \lambda < 800$ nm) in the solar spectrum is much more abundant (ca. 46 %). A use of visible light up to 600 nm increases the efficiency to 16 % and further improvement to 32 % is achievable if visible light use is extended to 800 nm (Kubacka et al. 2012; Linic et al. 2011; Paracchino et al. 2011; Serpone and Emeline 2012).

Currently, the efficiency for degradation of pollutants under visible-light irradiation is still low due to the fast charge recombination and backward reactions of photocatalysts (Chen et al. 2011). The efficient visible-light-driven photocatalysts requires closing the band gaps to harvest visible light in the long-wavelength regions as well as to improve the separation of photogenerated electrons (e^-) and holes (h^+) efficiently. Dopants into TiO_2 have been added to narrow the band gap in order for TiO_2 to be appropriate for absorbing visible light (Kamat 2012; Kubacka et al. 2012; Serpone et al. 2009). However, doped TiO_2 materials under visible light have lower chemical activity of surface active centers and decreased photoactivities compared to those formed under UV light irradiation (Serpone and Emeline 2012). Moreover, commonly used dopants are rare, expensive and/or toxic metals, which may not fulfill the principle of sustainable chemistry. Identification of suitable candidates capable of degrading pollutants under visible light is essential to provide clean remediation processes. The objective of this article is to provide information on the progress made in remediation of water using environmentally benign visible-light active iron-based oxides, ferrites.

Ferrites have a molecular formula M-Fe_2O_4 in which Fe_2O_3 is combined with a metal oxide (M-O). Ferrites may provide an alternative to TiO_2 because they have shown to be efficient in the visible light region (Han et al. 2007). Metals used in ferrites include Ca^{2+}, Zn^{2+}, Mg^{2+}, Ni^{2+}, Co^{2+}, and Mn^{2+} (Benko and Koffyberg 1986; Borse et al. 2008; Dom et al. 2011; Han et al. 2007; Tamaura et al. 1999). These ferrites, when prepared with a spinel structure, show promising photocatalytic activity (Kim et al. 2009). Spinel structures have the general formula AB_2X_4, where, in the case of ferrites, A is a metal, B is Fe^{3+} and X is oxygen (Burdett et al. 1982). As shown in Fig. 4.1 for example for $ZnFe_2O_4$, the spinel structure usually consists of both tetrahedral and octahedral sites, where the metal atoms occupy one-eighth of the tetrahedral sites and Fe^{3+} occupies one-half of the octahedral sites (Degueldre et al. 2009). The lattice parameter a and the cation-oxide distance R_{ZnO} and R_{FeO} in the octahedral and tetrahedral substructures were related by Eq. 4.1 (Degueldre et al. 2009)

$$A = 2(2)^{1/2}[R_{FeO}\cos(\psi/2) + R_{ZnO}\sin(\varphi/2)] \tag{4.1}$$

The tetrahedron internal angle (φ) and the octahedron equatorial angle (ψ) were identified as 109.471° and 95.375° for O-Zn-O and Fe-O-Fe, respectively.

The ferrites of Zn^{2+}, Ca^{2+}, and Mg^{2+} seem to be favorable as they are more relatively environmentally friendly. The energy diagram of these ferrites is shown in Fig. 4.2 (Dom et al. 2011). The band gaps of ~2.0 eV show the potential of ferrites to absorb visible light absorption and also the possibility for degrading pollutants in water (Casbeer et al. 2012; Hou et al. 2010; Ida et al. 2010; Li et al. 2011; Su et al. 2012).

The present chapter first describes briefly the synthesis and characterization of ferrites, followed by application of ferrites to degrade contaminants. Most of studies in literature have been performed on $ZnFe_2O_4$ and hence examples are presented using this form of ferrite.

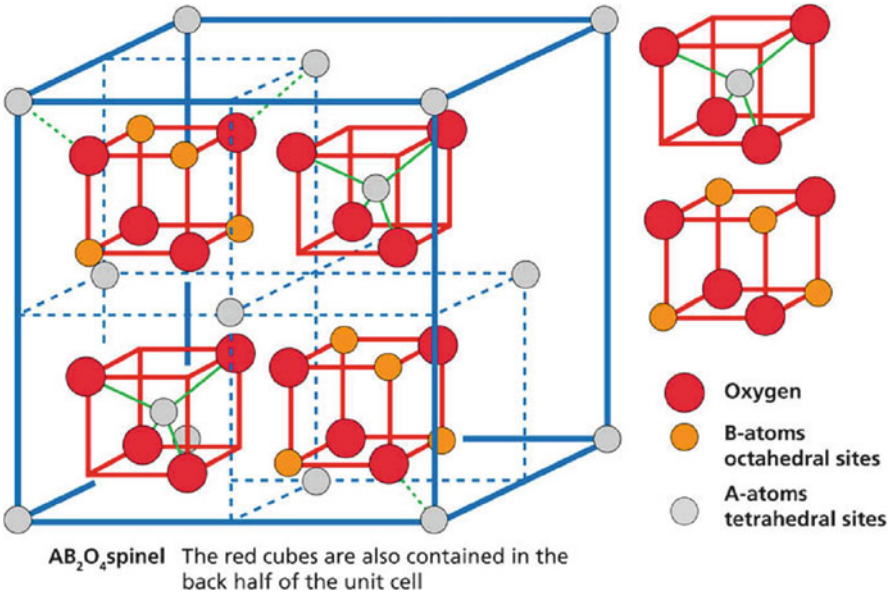

Fig. 4.1 Schematic description of the crystallographic structure for bulk $ZnFe_2O_4$. Occupied tetrahedral site in spinel sub-cell, Zn is *gray* and O is in *red*. Occupied octahedral site in spinel sub-cell, Fe is *yellow*, and O is in *red*. The arrangement in one unit cell with 3D succession of octahedral and tetrahedral sub-cells (Adapted from (Degueldre et al. 2009) with permission from Elsevier Ltd.)

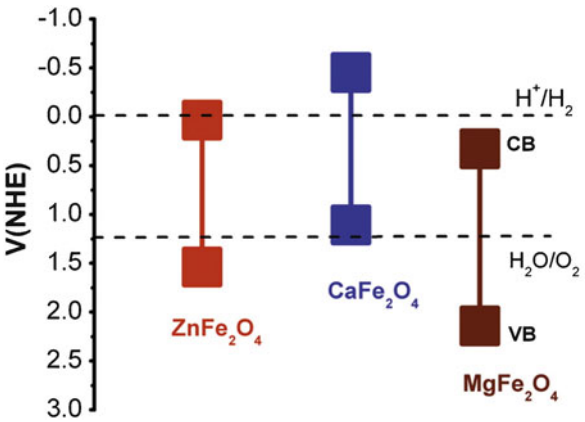

Fig. 4.2 Schematic diagram of MFe_2O_4 (M: Mg, Ca, Zn) showing the feasibility of materials as visible light photocatalysts. The thickness of the band edge (CB-*conduction*/VB *valence band*) indicates the possible variation in the value depending on various physico–chemical parameters of electrolyte and environmental conditions viz. *p*H, temperature, concentration etc. and there possible effects on the Fermi energy (Adapted from (Dom et al. 2011) with the permission of Elsevier Ltd.)

4.2 Synthesis of Ferrites

4.2.1 Spinel Ferrites

A number of methods used in synthesis of spinel ferrites are shown in Fig. 4.3. These method include thermal, sol-gel and citrate, co-precipitation, and solid-state reactions (Casbeer et al. 2012; Dom et al. 2011; Hou et al. 2011; Jadhav et al. 2012; Li et al. 2011; Pardeshi and Pawar 2011; Pradeep et al. 2011; Salunkhe et al. 2012; Su et al. 2012; Zhang et al. 2010a). In synthesis of ferrites, salts of Fe(III) and M(II) were used as precursors. Synthesis methods have recently been summarized (Casbeer et al. 2012). Highly visible-light active $ZnFe_2O_4$ nanotube array has also been prepared using sol-gel methods (Li et al. 2011). Microwave sintering process may be advantageous due to its shorter synthesis time compared to conventional methods (Dom et al. 2011).

4.2.2 Composite Ferrites

In composite ferrites, the emphasis has been on the coupling of titania and zinc ferrite through different approaches. Ferrite is sensitive to visible light while titania has high photoactivity (Chen et al. 2010; Cheng et al. 2004) and composites showed increased photocatalytic activity (Tan et al. 2012). Sol-gel and hydrothermal methods were successfully used to prepare either titania doped ferrite or ferrite

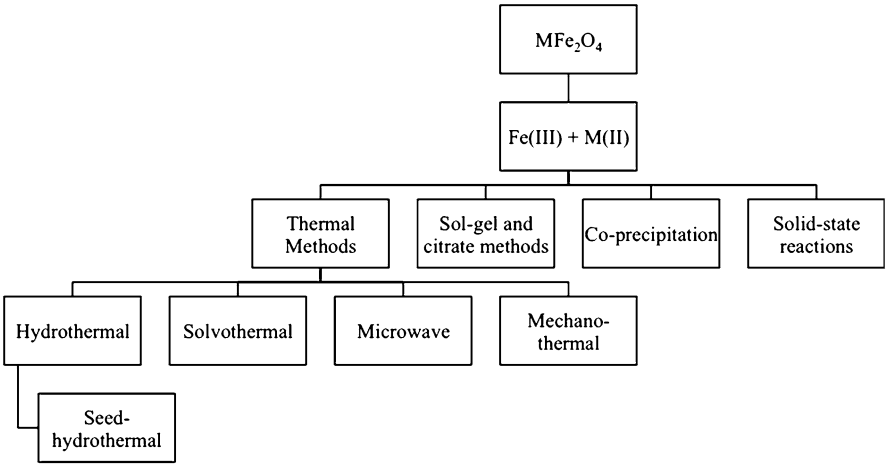

Fig. 4.3 Preparation methods of ferrites using Fe(III) and M(II) salts as precursors (Adapted from (Casbeer et al. 2012) with the permission of Elsevier Ltd)

doped titnia (Cheng et al. 2004; Liu et al. 2004; Moreira et al. 2012). More recently, TiO_2-$ZnFe_2O_4$ with an intermediate layer of alumina has been prepared by a multistep wet chemical method (Hankare et al. 2011). Other methods include the liquid catalytic phase transformation at low temperature and the two-step electrochemical processes (Hou et al. 2010; Shihong et al. 2009). Nanocomposites of $ZnFe_2O_4$ nanoplates and Ag nanoparticles and $ZnFe_2O_4$/multi-walled carbon nanotubes (MWCNTs) have also been prepared (Cao et al. 2011; Chen et al. 2010).

4.3 Characterization

Figure 4.4 shows the optical properties of ferrites, analyzed by UV–vis absorption spectroscopy. Ferrites have strong absorption in the visible range of 400–700 nm (Dom et al. 2011; Liu et al. 2009; Subramanian et al. 2004; Valenzuela et al. 2002). This is significant because of performing photocatalytic activity under visible light. Comparatively, TiO_2 does not show any significant absorption in the visible region. The electron excitation from the O-2p level into the Fe 3d level for ferrites may be causing absorption in the visible region (Lv et al. 2010). The two persistent absorption bands of spinel structures of nano $ZnFe_2O_4$ at $\nu_1 = 545$ and $\nu_2 = 292\ cm^{-1}$ in the Fourier Transform Infrared (FTIR) spectrum were observed (Pradeep et al. 2011). These bands could be related to the oxygen-metal cation complex presence in the tetrahedral and octahedral sites of the ferrite. Other surface techniques have also been applied to characterize ferrite, which include X-ray diffraction (XRD), X-ray spectroscopy (XAS), transmission electron microscopy (TEM), scanning electron microscopy (SEM), neutron diffraction analysis, and

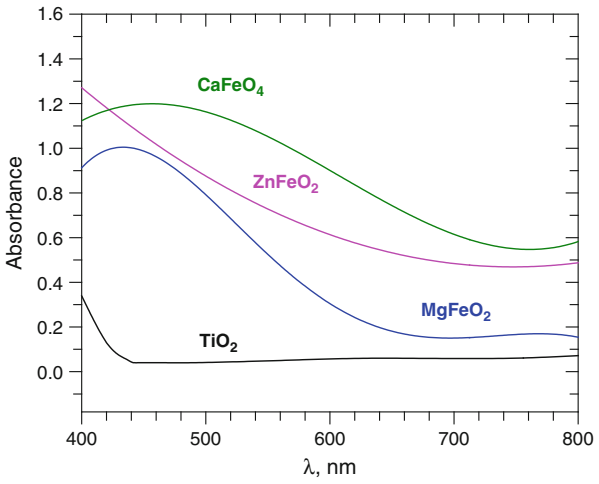

Fig. 4.4 Visible light spectra of metal ferrites (Adapted from (Dom et al. 2011; Liu et al. 2009; Subramanian et al. 2004; Valenzuela et al. 2002))

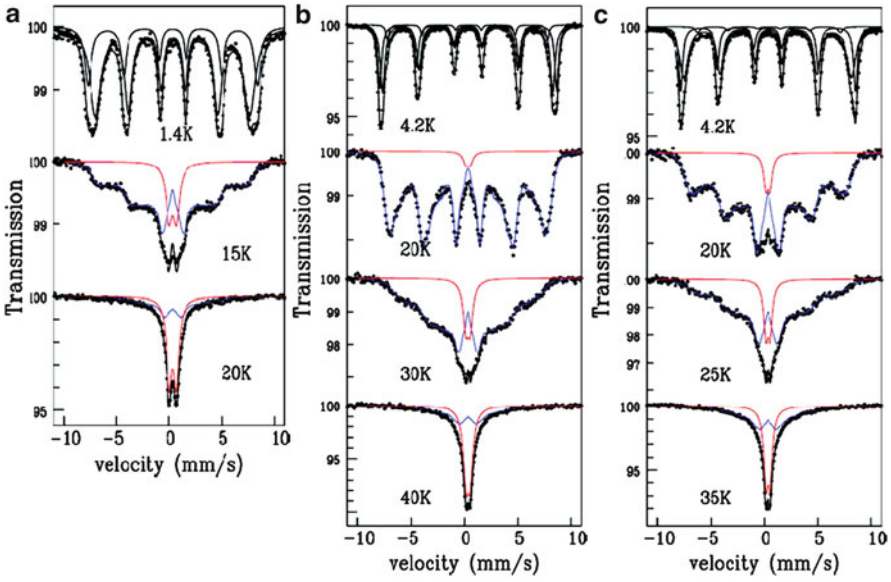

Fig. 4.5 Mössbauer spectra obtained at different temperatures for Z3 (**a**), Z11 (**b**), and Z19 (**c**) samples (Adapted from (Blanco-Gutiérrez et al. 2011) with the permission of the American Chemical Society)

Brunauer-Emmett-Teller (BET) surface area (Blanco-Gutierrez et al. 2011; Hankare et al. 2011; Hou et al. 2011; Li et al. 2011; Moreira et al. 2012; Nilsen et al. 2007).

Mossbauer spectroscopy has also been used to characterize $ZnFe_2O_4$ samples (Blanco-Gutiérrez et al. 2011). The zero-field Mossbauer spectra of samples, prepared differently are presented in Fig. 4.5 (Blanco-Gutiérrez et al. 2011). Samples Z3 and Z19 were synthesized using solvothermal method while Z11 was prepared by means of sol-gel method. All samples had different treatment time while temperature was ranged from 160 °C to 200 °C. Treatment times were 2 and 288 h for Z3 and Z19 samples, respectively. Sample Z11 was treated for 24 h. The mean particle sizes of samples were 3, 11, and 19 nm for Z3, Z11, and Z19, respectively. Spectra of samples at 1.4 and 4.2 K had two broadened sextets in which suggested the presence of Fe^{3+}. The non-Lorentzian shape of lines gave mean hypefine parameters as 47.2, 50.2, and 49.9 T for Z3, Z11, and Z19, respectively. The characteristic doublets appeared with increase in temperature (Fig. 4.5). This is indicative of superparamagnetic behavior of particles of such samples.

4.4 Oxidation by Ferrites

The absorption of light by semiconductor photocatalysis results in several processes (Fig. 4.6) (Teoh et al. 2012). In the first step, formation of electron–hole ($e\text{-}h^+$) occurs through bandgap excitation. A number of reactions can take place in absence

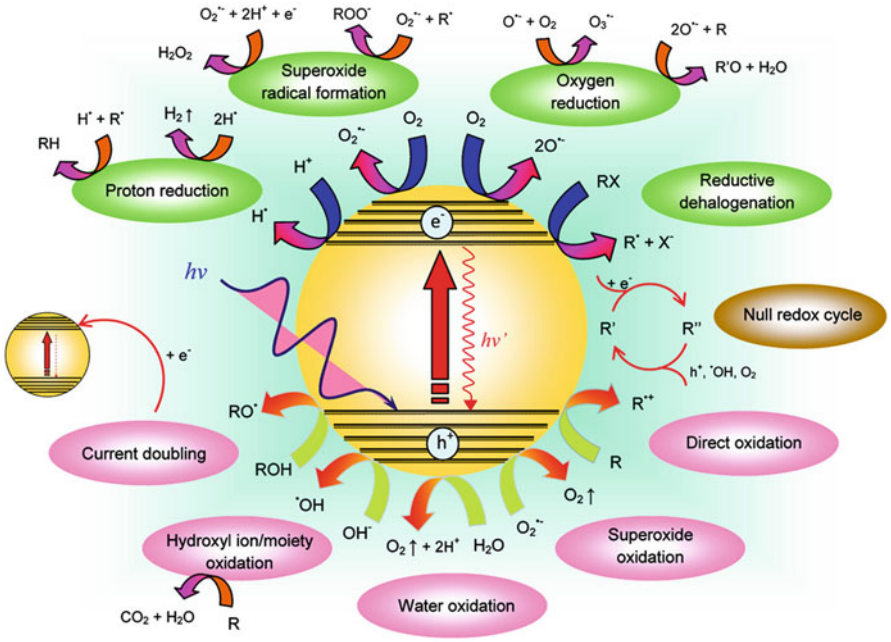

Fig. 4.6 Possible reaction pathways arising from the excitation of photocatalyst (Adapted from (Teoh et al. 2012) with the permission of American Chemical Society)

and presence of contaminants in water (Fig. 4.6). Both electron and hole can diffuse to the surfaces of semiconductors and reduce and oxidize the adsorbed contaminants, respectively (Fig. 4.6). Other possibility is the recombination of electron and hole, which decreases the efficiency of the photocatalysts to react with contaminants in water. Hydroxyl radicals ($^{\bullet}OH$) have been suggested to be dominated species to oxidize contaminants. Hydroxyl radicals are efficient in abstracting hydrogen atom and attaching to electron-rich moieties (Park and Choi 2005; Turchi and Ollis 1990). Superoxide species ($O_2^{\bullet-}$) are generated by the reaction of O_2 with electron (Gerischer and Heller 1991; Schwitzgebel et al. 1995). Other reactive oxygen species such as singlet oxygen ($^1O_2$), hydrogen peroxide (H_2O_2), and hydroperoxyl radicals ($HO_2^{\bullet}$) may also be produced and be involved in the photocatalytic oxidation reactions. In the next section, applications of ferrites (e.g., $ZnFe_2O_4$) as a photocatlysts in degrading contaminants are presented.

4.4.1 Degradation of Contaminants

Ferrites have been useful in decontamination of inorganic compounds and disinfection (Li et al. 2008; Liu et al. 1996; Rana et al. 2005; Rawat et al. 2007; Zhang et al. 2010b; Zhao et al. 2010). Examples include photodehydrogenation

Table 4.1 Degradation of phenols by ferrites

Contaminant	Catalyst	Irradiation	Reference
Phenol	Zn-Al ferrite	No	Xu et al. (2007)
4-Chlorophenol	$ZnFe_2O_4$-modified TiO_2 nanotube array electrode	Visible light	Hou et al. (2011)
4-Chlorophenol	$ZnFe_2O_4$ nanotube	Visible light	Li et al. (2011)
Phenol	$TiO_2/CoFe_2O_4$ composite	UV-visible light	Li et al. (2012)
2,4-Dichlorophenol	N-doped titania supported *on* $SrFe_{12}O_{19}$	Sunlight	Aziz et al. (2012b)
2,4-Dichlorophenol	TiO_2 nanocomposites/SiO_2 coating supported on $NiFe_2O_4$	Sunlight	Aziz et al. (2012a)
Phenol o-Nitrophenol p-Nitrophenol Picric acid	Multi-walled carbon nanotube supported on $NiFe_2O_4$	UV light	Xiong et al. (2012)

of H_2S using $ZnFe_2O_4$ and inactivation of *Escherichia coli* by composite ferrites, $Ag/MgFe_2O_4$, $Ag/Ni_2Fe_2O_4$, Ag/Zn_2FeO_4, and $Ag/CoFe_2O_4$. Ferrites have also shown effectiveness in degrading aliphatic compounds such as methanol, ethanol, isopropanol, acetaldehyde, oxalic acid, and butenes (Gibson and Hightower 1976; Manova et al. 2004, 2011; Shchukin et al. 2004; Tsoncheva et al. 2010). Most of studies on the remediation by ferrites are on the oxidation of phenols and dyes and are discussed below.

Phenols

A few studies on the oxidation of phenols by ferrites have been performed and are summarized in Table 4.1 (Aziz et al. 2012b; Hou et al. 2010; Li et al. 2012, 2011; Valenzuela et al. 2002; Xu et al. 2007). The concentrations of phenols in these studies were generally from 10 to 50 mg l^{-1}. These studies have demonstrated that phenols could be removed successfully using ferrite alone and composite ferrites. The current focus is on the composite ferrites to enhance the photocatalytic oxidation of phenols through synergistic effects. The presence of ferrites in the TiO_2-ferrite composite not only increases absorbance of visible light, but also increases absorbance in the UV light in order to assist photooxidation of phenol (Li et al. 2012, 2011). Furthermore, composites could be magnetically separated (Aziz et al. 2012a, b; Li et al. 2012). The photocatalytic oxidation of phenols using a magnetically recyclable photocatalyst, multi-walled carbon nanotubes (MWNT) supported $NiFe_2O_4$ is shown in Fig. 4.7 (Xiong et al. 2012). Figure 4.7a shows the degradation of phenol using $NiFe_2O_4$/MWNT nanocomposites having different MWNT content. The degradation of phenols increased with increasing amount of MWNT in the nanocomposites, however, the degradation rate had no such relationship. The degradation of phenol under UV radiation followed pseudo-first-order kinetics and obtained rate constant (k) as a function of content of MWNT are

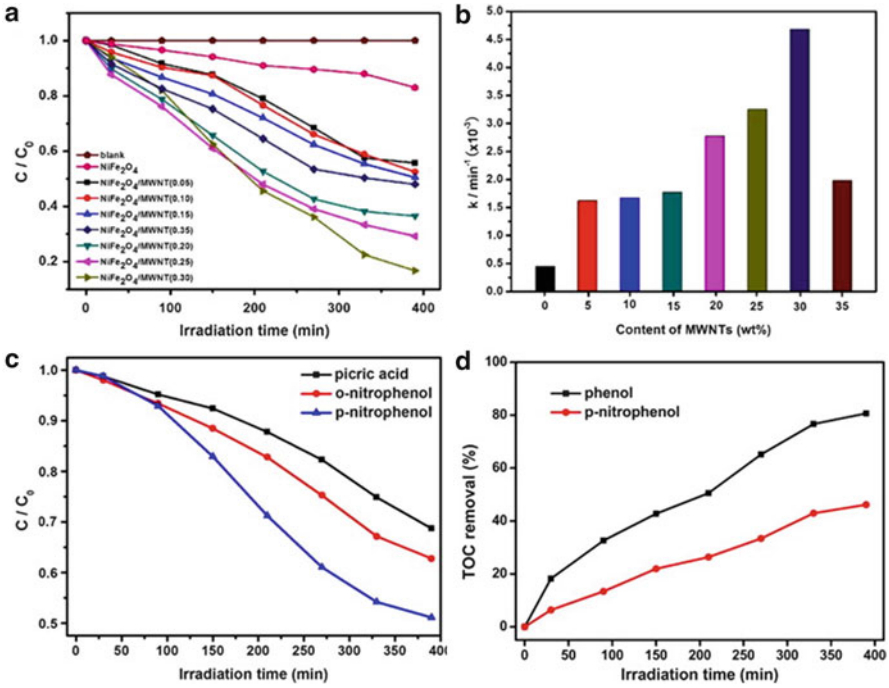

Fig. 4.7 (**a**) Photocatalytic degradation of phenol by $NiFe_2O_4$/multi-walled carbon nanotubes (MWNT) photocatalysts with differing MWNT contents under UV light irradiation; (**b**) The pseudo-first-order rate constant *k* as a function of MWNT content; (**c**) Photocatalytic degradation of nitrophenols (o-nitrophenol, p-nitrophenol, picric acid) by $NiFe_2O_4$/MWNT(0.30) nanocomposite photocatalysts under UV light irradiation; (**d**) Evolution of TOC removal of phenol and p-nitrophenol with irradiation time (Adapted from (Xiong et al. 2012) with the permission of Elsevier Ltd.)

shown in Fig 4.7b. $NiFe_2O_4$/MWNT nanocomposite with 30 wt % MWNT exhibited the best photocatalytic activity. Degradation of picric acid, o-nitrophenol, and p-nitrophenol are shown in Fig. 4.7c. Most of the phenol degraded significantly under UV light in 400 min. This study also determined the total organic carbon (TOC) for the degradation of phenol and p-nitrophenol (Fig. 4.7d). Removals of TOC were ~80 % and ~40 % for phenol and p-nitrophenol, respectively. Incomplete removal of TOC suggests that the oxidation of phenol and p-nitrophenol resulted in simple organic compounds in the $NiFe_2O_4$/MWNT/UV radiation (Xiong et al. 2012).

Dyes

Numerous studies on the oxidation of degradation of dyes by ferrites alone and composite ferrites have been carried out (Baldrian et al. 2006; Casbeer et al. 2012; Li et al. 2011; Moreira et al. 2012). Dyes studied include methyl orange (MO),

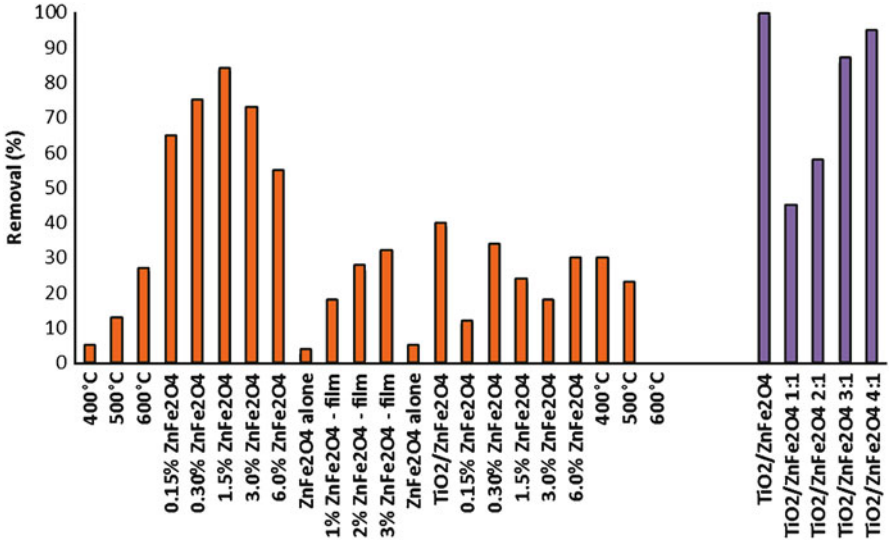

Fig. 4.8 Degradation of methyl orange (MO) and rhodamine B (RhB) dyes by $TiO_2/ZnFe_2O_4$ composite photocatalysts. All listed reactions contain the composite unless otherwise noted. MO solutions irradiated with visible light, while RhB solutions are irradiated with UV light (Adapted from (Casbeer et al. 2012) with the permission of Elsevier Ltd.)

methylene blue (MB), rhodamine B (RhB), bromophenol blue, Chicago sky blue, eosine yellow, evans blue, naphthol blue black, phenol red, poly B-411, and reactive orange 16. The concentration levels of dyes were usually in the range of 50–500 mg L^{-1}. In a recent work, results of the studies have been summarized (Casbeer et al. 2012). Ferrites as photocatalyst alone were effective in degrading dyes, but the efficiency of degradation was enhanced when ferrites were used as composite photocatalysts. This is shown in Fig. 4.8. The degradation of RhB by ferrites was examined by UV light while visible light was applied in irradiating the MO dye. The temperature of ferrite synthesis influenced the degradation of RhB. Increase in the amount of TiO_2 in the composite ferrites increased the degradation efficiency of dyes (Fig. 4.8). Decrease in crystal size of ferrites also increased the degradation efficiency of dyes (Fan et al. 2009).

In a recent work, the photocatalytic degradation of acid orange II (AOII) was studied by combining $ZnFe_2O_4$ with H_2O_2 under visible light ($\lambda > 400$ nm) (Su et al. 2012). Significantly direct photolysis of AOII by visible light was difficult, but oxidation of AOII was possible due to generation of $^{\bullet}OH$ radicals in the system (Fig. 4.9). The Fenton-type reaction can produce $^{\bullet}OH$ radicals (Path A). The formation of $^{\bullet}OH$ radicals is also due to oxidation of water by holes on the surface of the ferrite (Path B). The capture of electron by H_2O_2 gives $^{\bullet}OH$ radicals (Path C). The Path C is advantageous because it decreases the recombination of electron and hole and hence enhance the formation of $^{\bullet}OH$ radicals. The mechanism of the reactions was examined by adding scavengers of reactive species, oxalate,

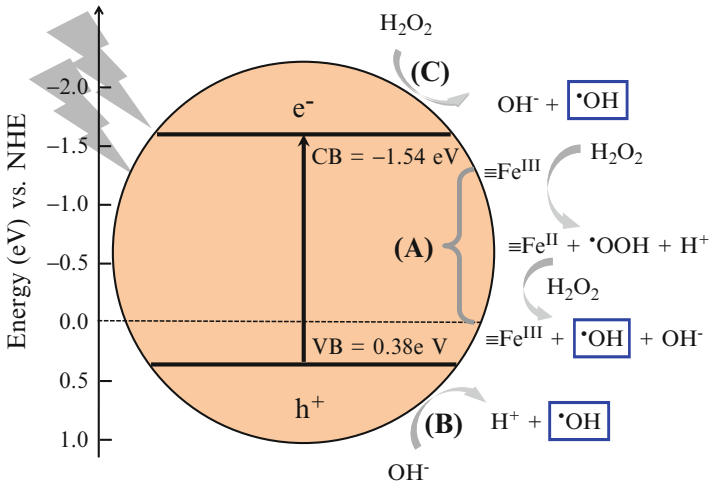

Fig. 4.9 A hypothetical scheme for the generation of OH radical in H_2O_2-$ZnFe_2O_4$-visible light system (Adapted from (Su et al. 2012) with the permission of Elsevier Ltd.)

iso-propoanol, Cr(VI), and KI, into the system. Degradation rate did not show any influence by adding oxalate. This suggests that oxidation of AOII by hole was less likely to be involved because hole is highly reactive with oxalate. Cr(VI) can react rapidly with electron and the degradation rate decreases in the presence of Cr(VI), which suggest that electron formed at the surface of the ferrite is involved. Both iso-propoanol and KI are good scavengers of •OH radicals and degradation of AOI decreased very significantly. This confirmed the dominant role of the •OH radicals in degradation of AOII. Basically, Paths, A, B, and C enhanced the degradation of AOII (Su et al. 2012). Degradation of AOII in the $ZnFe_2O_4/H_2O_2$/visible light was almost complete within 2 h. The amount of $ZnFe_2O_4$ and the concentration of H_2O_2 influenced the degradation of AOII.

4.5 Conclusion

$ZnFe_2O_4$-mediated photocatalytic oxidation of organic contaminations is a promising alternative technology for remediation of contaminants in water treatment. Pioneering works indicate that $ZnFe_2O_4$ possesses a relatively low visible-light-driven activity for organic pollutants, however, the technology is a potentially economical and benign process due to its capability to absorb the visible light of solar energy, stability against photo- and chemical- corrosion, low cost, and non-toxicity. In this case, it is still a challenge to explore the highly-efficient modified ferrites for remediation of contaminants under visible light. The size and morphology control of ferrites is one of the most important approaches that

can enhance the photocatalytic activity. Compared with a traditional synthesized method, i.e. co-precipitation and sol-gel techniques, resulting in large particles and a broad size distribution, some innovative methods should be developed which can synthesize smaller size $ZnFe_2O_4$. An alternative promising approach is to modify ferrites with an appropriate matching-band-gap-energy semiconductor in a way that the photogenerated e^-/h^+ can be transferred between ferrites and matching-band-gap-energy semiconductor. This effective charge suppresses the combination of the photoinduced electrons and holes, which is beneficial to improve the photocatalytic efficiency. Further improvement in the modification of ferrites and ferrite composite for photocatalytic degradation of organic pollutants is still needed.

Acknowledgements V.K. Sharma and D.D. Dionysiou acknowledge support from the National Science Foundation grant (CBET 1236331) for ferrite research. C. He wishes to thank the National Natural Science Foundation of China (No. 20877025), National Natural Science Foundation of Guangdong Province (No. S2011010001836) and the Fundamental Research Funds for the Central Universities (No. 09lgpy20).

References

Abe R (2011) Development of a new system for photocatalytic water splitting into H_2 and O_2 under visible light irradiation. Bull Chem Soc Jpn 84:1000–1030

Aziz AA, Cheng CK, Ibrahim S, Matheswaran M, Saravanan P (2012a) Visible light improved, photocatalytic activity of magnetically separable titania nanocomposite. Chem Eng J 183:349–356

Aziz AA, Yong KS, Ibrahim S, Pichiah S (2012b) Enhanced magnetic separation and photocatalytic activity of nitrogen doped titania photocatalyst supported on strontium ferrite. J Hazard Mater 199–200:143–150

Baldrian P, Merhautová V, Gabriel J, Nerud F, Stopka P, Hrubý M, Beneš MJ (2006) Decolorization of synthetic dyes by hydrogen peroxide with heterogeneous catalysis by mixed iron oxides. Appl Catal Environ 66:258–264

Benko FA, Koffyberg FP (1986) The effect of defects on some photoelectrochemical properties of semiconducting $MgFe_2O_4$. Mater Res Bull 21:1183–1188

Blanco-Gutierrez V, Climent-Pascual E, Torralvo-Fernandez MJ, Saez-Puche R, Fernandez-Diaz MT (2011) Neutron diffraction study and superparamagnetic behavior of $ZnFe_2O_4$ nanoparticles obtained with different conditions. J Solid State Chem 184:1608–1613

Blanco-Gutiérrez V, Jiménez-Villacorta F, Bonville P, Torralvo-Fernández MJ, Sáez-Puche R (2011) X-ray absorption spectroscopy and Mössbauer spectroscopy studies of superparamagnetic $ZnFe_2O_4$ nanoparticles. J Phys Chem C 115:1627–1634

Borse PH, Jun H, Choi SH, Hong SJ, Lee JS (2008) Phase and photoelectrochemical behavior of solution-processed Fe_2O_3 nanocrystals for oxidation of water under solar light. Appl Phys Lett 93

Burdett JK, Price GD, Price SL (1982) Role of the crystal-field theory in determining the structures of spinels. J Am Chem Soc 104:92–95

Cao J, Kako T, Li P, Ouyang S, Ye J (2011) Fabrication of p-type $CaFe_2O_4$ nanofilms for photoelectrochemical hydrogen generation. Electrochem Commun 13:275–278

Casbeer E, Sharma VK, Li X (2012) Synthesis and photocatalytic activity of ferrites under visible light: a review. Sep Purif Technol 87:1–14

Chen C-H, Liang Y-H, Zhang W-D (2010) $ZnFe_2O_4$/MWCNTs composite with enhanced photocatalytic activity under visible-light irradiation. J Alloys Compd 501:168–172

Chen X, Liu L, Yu PY, Mao SS (2011) Increasing solar absorption for photocatalysis with black hydrogenated titanium dioxide nanocrystals. Science 331:746–750

Cheng P, Li W, Zhou T, Jin Y, Gu M (2004) Physical and photocatalytic properties of zinc ferrite doped titania under visible light irradiation. J Photochem Photobiol A 168:97–101

Degueldre C, Kuri G, Borca CN, Grolimund D (2009) X-ray micro- fluorescence, diffraction and absorption spectroscopy for local structure investigation of a radioactive zinc ferrite deposit. Corros Sci 51:1690–1695

Di Paola A, García-López E, Marcì G, Palmisano L (2012) A survey of photocatalytic materials for environmental remediation. J Hazard Mater 211–212:3–29

Dom R, Subasri R, Radha K, Borse PH (2011) Synthesis of solar active nanocrystalline ferrite, MFe_2O_4 (M: Ca, Zn, Mg) photocatalyst by microwave irradiation. Solid State Commun 151:470–473

Fan G, Gu Z, Yang L, Li F (2009) Nanocrystalline zinc ferrite photocatalysts formed using the colloid mill and hydrothermal technique. Chem Eng J 155:534–541

Gerischer H, Heller A (1991) The role of oxygen in photooxidation of organic molecules on semiconductor particles. J Phys Chem 95:5261–5267

Gibson MA, Hightower JW (1976) Oxidative dehydrogenation of butenes over magnesium ferrite kinetic and mechanistic studies. J Catal 41:420–430

Han SB, Kang TB, Joo OS, Jung KD (2007) Water splitting for hydrogen production with ferrites. Sol Energ 81:623–628

Hankare PP, Patil RP, Jadhav AV, Garadkar KM, Sasikala R (2011) Enhanced photocatalytic degradation of methyl red and thymol blue using titania-alumina-zinc ferrite nanocomposite. Appl Catal Environ 107:333–339

Hoffmann MR, Martin ST, Choi W, Bahnemann DW (1995) Environmental applications of semiconductor photocatalysis. Chem Rev 95:69–96

Hou X, Feng J, Liu X, Ren Y, Fan Z, Wei T, Meng J, Zhang M (2011) Synthesis of 3D porous ferromagnetic $NiFe_2O_4$ and using as novel adsorbent to treat wastewater. J Colloid Interface Sci 362:477–485

Hou Y, Li X, Zhao Q, Quan X, Chen G (2010) Electrochemically assisted photocatalytic degradation of 4-chlorophenol by $ZnFe_2O_4$-modified TiO_2 nanotube array electrode under visible light irradiation. Environ Sci Technol 44:5098–5103

Ida S, Yamada K, Matsunaga T, Hagiwara H, Matsumoto Y, Ishihara T (2010) Preparation of p-type $CaFe_2O_4$ photocathodes for producing hydrogen from water. J Am Chem Soc 132:17343–17345

Jadhav SV, Jinka KM, Bajaj HC (2012) Nanosized sulfated zinc ferrite as catalyst for the synthesis of nopol and other fine chemicals. Catal Today 198:98–105

Kamat PV (2012) Manipulation of charge transfer across semiconductor interface. A criterion that cannot be ignored in photocatalyst design. J Phys Chem Lett 3:663–672

Kim HG, Borse PH, Jang JS, Jeong ED, Jung O, Suh YJ, Lee JS (2009) Fabrication of $CaFe_2O_4$/$MgFe_2O_4$ bulk heterojunction for enhanced visible light photocatalysis. Chem Commun 39:5889–5891

Kubacka A, Fernández-García M, Colón G (2012) Advanced nanoarchitectures for solar photocatalytic applications. Chem Rev 112:1555–1614

Li C-J, Wang JN, Wang B, Gong JR, Lin Z (2012) Direct formation of reusable TiO_2/$CoFe_2O_4$ heterogeneous photocatalytic fibers via two-spinneret electrospinning. J Nanosci Nanotechnol 12:2496–2502

Li S, Wang E, Tian C, Mao B, Kang Z, Li Q, Sun G (2008) Jingle-bell-shaped ferrite hollow sphere with a noble metal core: simple synthesis and their magnetic and antibacterial properties. J Solid State Chem 181:1650–1658

Li X, Hou Y, Zhao Q, Teng W, Hu X, Chen G (2011) Capability of novel $ZnFe_2O_4$ nanotube arrays for visible-light induced degradation of 4-chlorophenol. Chemosphere 82:581–586

Li Y, Liu Z (2011) Particle size, shape and activity for photocatalysis on titania anatase nanoparticles in aqueous surroundings. J Am Chem Soc 133:15743–15752

Linic S, Christopher P, Ingram DB (2011) Plasmonic-metal nanostructures for efficient conversion of solar to chemical energy. Nat Mater 10:911–921

Liu G-G, Zhang X-Z, Xu Y-J, Niu X-S, Zheng L-Q, Ding X-J (2004) Effect of $ZnFe_2O_4$ doping on the photocatalytic activity of TiO_2. Chemosphere 55:1287–1291

Liu J, Lu G, He H, Tan H, Xu T, Xu K (1996) Studies on photocatalytic activity of zinc ferrite catalysts syntedesized by shock waves. Mater Res Bull 31:1049–1056

Liu Z, Zhao Z, Miyauchi M (2009) Efficient visible light active $CaFe_2O_4/WO_3$ based composite photocatalysts: effect of interfacial modification. J Phys Chem C 113:17132–17137

Lv H, Ma L, Zeng P, Ke D, Peng T (2010) Synthesis of floriated $ZnFe_2O_4$ with porous nanorod structures and its photocatalytic hydrogen production under visible light. J Mater Chem 20:3665–3672

Manova E, Tsoncheva T, Paneva D, Mitov I, Tenchev K, Petrov L (2004) Mechanochemically synthesized nano-dimensional iron-cobalt spinel oxides as catalysts for methanol decomposition. Appl Catal Gen 277:119–127

Manova E, Tsoncheva T, Paneva D, Popova M, Velinov N, Kunev B, Tenchev K, Mitov I (2011) Nanosized copper ferrite materials: mechanochemical synthesis and characterization. J Solid State Chem 184:1153–1158

Moreira E, Fraga LA, Mendonça MH, Monteiro OC (2012) Synthesis, optical, and photocatalytic properties of a new visible-light-active $ZnFe_2O_4$-TiO_2 nanocomposite material. J Nanopart Res 14:1–10

Nilsen MH, Nordhei C, Ramstad AL, Nicholson DG, Poliakoff M, Cabanas A (2007) XAS (XANES and EXAFS) investigations of nanoparticulate ferrites synthesized continuously in near critical and supercritical water. J Phys Chem C 111:6252–6262

Paracchino A, Laporte V, Sivula K, Grätzel M, Thimsen E (2011) Highly active oxide photocathode for photoelectrochemical water reduction. Nat Mater 10:456–461

Pardeshi SK, Pawar RY (2011) $SrFe_2O_4$ complex oxide an effective and environmentally benign catalyst for selective oxidation of styrene. J Mol Catal A Chem 334:35–43

Park H, Choi W (2005) Photocatalytic conversion of benzene to phenol using modified TiO_2 and polyoxometalates. Catal Today 101:291–297

Pradeep A, Priyadharsini P, Chandrasekaran G (2011) Structural, magnetic and electrical properties of nanocrystalline zinc ferrite. J Alloys Compd 509:3917–3923

Qu X, Brame J, Li Q, Alvarez PJJ (2012) Nanotechnology for a safe and sustainable water supply: enabling integrated water treatment and reuse. Acc Chem Res 45. doi: 10.1021/ar300029v

Rajeshwar K (2011) Solar energy conversion and environmental remediation using inorganic semiconductor-liquid interfaces: the road traveled and the way forward. J Phys Chem Lett 2:1301–1309

Rajeshwar K, De Tacconi NR, Timmaji HK (2012) New-generation oxide semiconductors for solar energy conversion and environmental remediation. J Nano Res 17:185–191

Rana S, Rawat J, Misra RDK (2005) Anti-microbial active composite nanoparticles with magnetic core and photocatalytic shell: TiO_2-$NiFe_2O_4$ biomaterial system. Acta Biomater 1:691–703

Rawat J, Rana S, Srivastava R, Misra RDK (2007) Antimicrobial activity of composite nanoparticles consisting of titania photocatalytic shell and nickel ferrite magnetic core. Mater Sci Eng C 27:540–545

Salunkhe AB, Khot VM, Phadatare MR, Pawar SH (2012) Combustion synthesis of cobalt ferrite nanoparticles – influence of fuel to oxidizer ratio. J Alloys Compd 514:91–96

Schwitzgebel J, Ekerdt JG, Gerischer H, Heller A (1995) Role of the oxygen molecule and of the photogenerated electron in TiO_2-photocatalyzed air oxidation reactions. J Phys Chem 99:5633–5638

Serpone N, Emeline AV (2012) Semiconductor photocatalysis – past, present, and future outlook. J Phys Chem Lett 3:673–677

Serpone N, Emeline AV, Horikoshi S (2009) Photocatalysis and solar energy conversion (chemical aspects). Photochemistry 37:300–361

Serpone N, Emeline AV, Horikoshi S, Kuznetsov VN, Ryabchuk VK (2012) On the genesis of heterogeneous photocatalysis: a brief historical perspective in the period 1910 to the mid-1980s. Photochem Photobiol Sci 11:1121–1150

Shchukin DG, Ustinovich EA, Sviridov DV, Kulak AI (2004) Titanium and iron oxide-based magnetic photocatalysts for oxidation of organic compounds and sulfur dioxide. High Energ Chem 38:167–173

Shihong X, Daolun F, Wenfeng S (2009) Preparations and photocatalytic properties of visible-light-active zinc ferrite-doped TiO_2 photocatalyst. J Phys Chem C 113:2463–2467

Su M, He C, Sharma VK, Abou Asi M, Xia D, Li X-Z, Deng H, Xiong Y (2012) Mesoporous zinc ferrite: synthesis, characterization, and photocatalytic activity with H_2O_2/visible light. J Hazard Mater 211–212:95–103

Subramanian V, Wolf EE, Kamat PV (2004) Catalysis with TiO_2/Gold nanocomposites. Effect of metal particle size on the fermi level eqilibration. J Am Chem Soc 126:4943–4950

Tamaura Y, Ueda Y, Matsunami J, Hasegawa N, Nezuka M, Sano T, Tsuji M (1999) Solar hydrogen production by using ferrites. Sol Energ 65:55–57

Tan D, Bi D, Shi P, Xu S (2012) Preparation and photocatalytic property of TiO_2/NiFe $_2O_4$ composite photocatalysts. Adv Mater Res 518–523:775–779

Tao J, Luttrell T, Batzill M (2011) A two-dimensional phase of TiO_2 with a reduced bandgap. Nat Chem 3:296–300

Teoh WY, Scott JA, Amal R (2012) Progress in heterogeneous photocatalysis: from classical radical chemistry to engineering nanomaterials and solar reactors. J Phys Chem Lett 3:629–639

Tsoncheva T, Manova E, Velinov N, Paneva D, Popova M, Kunev B, Tenchev K, Mitov I (2010) Thermally synthesized nanosized copper ferrites as catalysts for environment protection. Catal Commun 12:105–109

Turchi CS, Ollis DF (1990) Photocatalytic degradation of organic water contaminants: mechanisms involving hydroxyl radical attack. J Catal 122:178–192

Valenzuela MA, Bosch P, Jimenez-Becerrill J, Quiroz O, Paez AI (2002) Preparation, characterization and photocatalytic activity of ZnO, Fe_2O_3 and $ZnFe_2O_4$. J Photochem Photobiol A 148:177–182

WHO (2010) UNICEF Progress on sanitation and drinking-water 2010 update

Xiong P, Fu Y, Wang L, Wang X (2012) Multi-walled carbon nanotubes supported nickel ferrite: a magnetically recyclable photocatalyst with high photocatalytic activity on degradation of phenols. Chem Eng J 195–196:149–157

Xu A, Yang M, Qiao R, Du H, Sun C (2007) Activity and leaching features of zinc-aluminum ferrites in catalytic wet oxidation of phenol. J Hazard Mater 147:449–456

Zhang G-Y, Sun Y-Q, Gao D-Z, Xu Y-Y (2010a) Quasi-cube $ZnFe_2O_4$ nanocrystals: hydrothermal synthesis and photocatalytic activity with TiO_2 (Degussa P25) as nanocomposite. Mater Res Bull 45:755–760

Zhang S, Niu H, Cai Y, Zhao X, Shi Y (2010b) Arsenite and arsenate adsorption on coprecipitated bimetal oxide magnetic nanomaterials: $MnFe_2O_4$ and $CoFe_2O_4$. Chem Eng J 158:599–607

Zhao L, Li X, Zhao Q, Qu Z, Yuan D, Liu S, Hu X, Chen G (2010) Synthesis, characterization and adsorptive performance of $MgFe_2O_4$ nanospheres for SO_2 removal. J Hazard Mater 184:704–709